BMC Cancer

RESEARCH Open Access

A CT-based radiomics model for predicting progression-free survival in patients with epithelial ovarian cancer

Yinping Leng[1,2], Jingjing Zhou[1,2], Wenjie Liu[1,2], Fengyuan Luo[1,2], Fei Peng[3†] and Lianggeng Gong[1,2*†]

Abstract

Purpose This study aimed to develop and validate a CT-based radiomics nomogram for predicting the progression-free survival (PFS) of epithelial ovarian cancer (EOC).

Materials and methods A total of 144 EOC patients were retrospectively enrolled from two hospitals and The Cancer Genome Atlas and The Cancer Imaging Archive, divided into a training set ($n=101$) and a test set ($n=43$) using a 7:3 ratio. Radiomic features were extracted from contrast enhanced CT images. The radiomics score (rad-score) was developed using the least absolute shrinkage and selection operator (LASSO) Cox regression. Clinical semantic features with $P<0.05$ in multivariate Cox regression were combined with rad-score to develop radiomics nomogram. The predictive performance of the nomogram was assessed using the concordance index (C-index) and calibration curves.

Results Multivariate Cox regression analysis revealed that the International Federation of Obstetrics and Gynecology stage and residual tumor are significant predictors of PFS. Twelve radiomic features were selected by LASSO Cox regression. The combined model demonstrated superior predictive performance, with a C-index of 0.78 (95% CI: 0.689–0.889) in the training set, and 0.73 (95% CI: 0.572–0.886) in the test set. The combined model outperformed the clinical and radiomics models in predicting 1-, 3-, and 5-year PFS, with area under curves of 0.850 (95% CI: 0.722–0.943), 0.828 (95% CI: 0.722–0.901), and 0.845 (95% CI: 0.722–0.943), respectively. Calibration curves of the radiomic nomogram for prediction of 1-year, 3-year, 5-year PFS showed excellent calibrations in both training and test sets.

Conclusion The combined model integrating rad-score and clinical semantic features effectively evaluates PFS in EOC patients. The radiomics nomogram provides a non-invasive, simple, and feasible method to predict PFS in EOC patients, which may facilitate clinical decision-making.

Keywords Epithelial ovarian cancer, CT, Radiomics, Progression-free survival, Nomogram

†Fei Peng and Lianggeng Gong contributed equally to this work.

*Correspondence:
Lianggeng Gong
gong111999@126.com

[1]Department of Radiology, The Second Affiliated Hospital, Jiangxi Medical College, Nanchang University, Minde Road No. 1, Nanchang, Jiangxi Province 330006, China
[2]Jiangxi Provincial Key Laboratory of Intelligent Medical Imaging, Nanchang, China
[3]Department of Radiology, The First Affiliated Hospital, Hengyang Medical School, University of South China, Hengyang, China

Background

Ovarian cancer is the main cause of death from gynecological cancer, and shows an increasing trend in mortality [1, 2]. Epithelial ovarian cancer (EOC) is the leading gynecological malignancy, responsible for more than 70% of ovarian cancer fatalities [3]. 80% of EOC patients can achieve complete clinical remission through tumor cell reduction surgery and cisplatin based chemotherapy [4]. About 25% of advanced-stage EOC patients experience recurrence within 6 months, and ultimately over 70% of patients experience recurrence within 3 years [5, 6]. The median progress-free survival (PFS) is only 18 months. Therefore, predicting the recurrence and progression of EOC patients is crucial for monitoring disease progression and guiding personalized treatment.

Serum biomarkers, such as carcinoma antigen 125 (CA125) and human epididymis protein 4, have potential as predictive indicators for EOC recurrence [7, 8]. However, their limited specificity poses a challenge in adequately meeting clinical requirements. Computed tomography (CT) is recommended by both the European Society of Urogenital Radiology and the American Society of Radiology for preoperative staging and follow-up of EOC [9, 10]. Contrast-enhanced CT, a commonly utilized diagnostic tool, offers a non-invasive and cost-effective approach for obtaining prognostic information on EOC [11]. The diagnosis of EOC using CT largely depends on the experience of radiologists, leading to subjective judgments based on tumor size, density, and relationships with surrounding tissues. This reliance on subjective interpretation results in a lack of objectivity. Therefore, there is a critical need to identify new biomarkers to guide clinical decision-making and enhance patient outcomes.

Radiomics can quantify the pixel and spatial distribution relationships in traditional CT images, fully explore hidden information that cannot be observed by the naked eye, describe tumor phenotype and heterogeneity from a macro perspective, and provide new methods for tumor diagnosis and prognosis evaluation [12–14]. Numerous studies have highlighted the prognostic significance of CT radiomics across different cancer types, such as non-small cell lung cancer [15], pancreatic ductal adenocarcinoma [16], and osteosarcoma [17]. Rizzo et al. found that CT-based radiomics features can predict the 12-month disease progression risk in ovarian cancer patients [18]. Although radiomics has demonstrated potential in predicting the prognosis of EOC, existing studies are predominantly based on single-center cohorts. As a result, the performance of these models tends to degrade significantly when validated across multiple institutions. Our study utilized a multicenter approach to develop a predictive model that integrates radiomics and clinical semantic features for predicting PFS in EOC patients. We also created a nomogram as a non-invasive tool to aid in developing personalized treatment plans for EOC patients.

Methods

Patients

The Institutional Review Committee of the participating hospitals approved this retrospective study, waiving the requirement for informed consent. We included EOC patients identified from a public database (The Cancer Genome Atlas and The Cancer Imaging Archive, TCGA-TCIA) and two medical hospitals (April 2017 to December 2020). The inclusion criteria were as follows: patients confirmed by histopathology; patients received standard treatment (tumor cell reduction surgery and 6–8 cycles of platinum based chemotherapy); patients underwent enhanced CT scan before surgery. The exclusion criteria were as follows: patients with treatment before CT examination; patients with poor CT image quality; patients with incomplete clinical pathological data or follow-up information. The specific enrollment process of the patient is shown in Fig. 1. Finally, a total of 144 EOC patients were enrolled in this study. The patient distribution across centers is detailed in Supplementary A1. In order to avoid potential overfitting caused by a small amount of data, all patients of the three centers were randomly divided into a training set ($n = 101$) and a test set ($n = 43$) at a ratio of 7:3. The clinical characteristics includes age, menopausal status, International Federation of Gynecology and Obstetrics (FIGO) stage, preoperative CA125 level, and residual tumor (> 1 cm).

Follow-Up and clinical endpoints

All patients were followed up every 3 months for the first 2 years, then every 6 months for the following 3–5 years, then annually after 5 years. The deadline for follow-up is December 2023. Serum CA125 level, physical exam, and CT examination were used to evaluate recurrence or progression of tumors. The endpoint event of this study is tumor recurrence or progression, which was diagnosed based on clinical symptoms, rising CA125 levels, and radiological findings. PFS is defined as the time interval from the first day following cytoreductive surgery until the occurrence of tumor progression, death from any cause, or the date of the last follow-up.

CT images acquisition and CT semantic features interpretation

The CT protocol for patients from TCGA-TCIA is unavailable; however, the reconstructed slice thicknesses were determined to be 2.5 mm and/or 1.25 mm based on the downloaded images. CT examinations were conducted on patients from two hospitals using

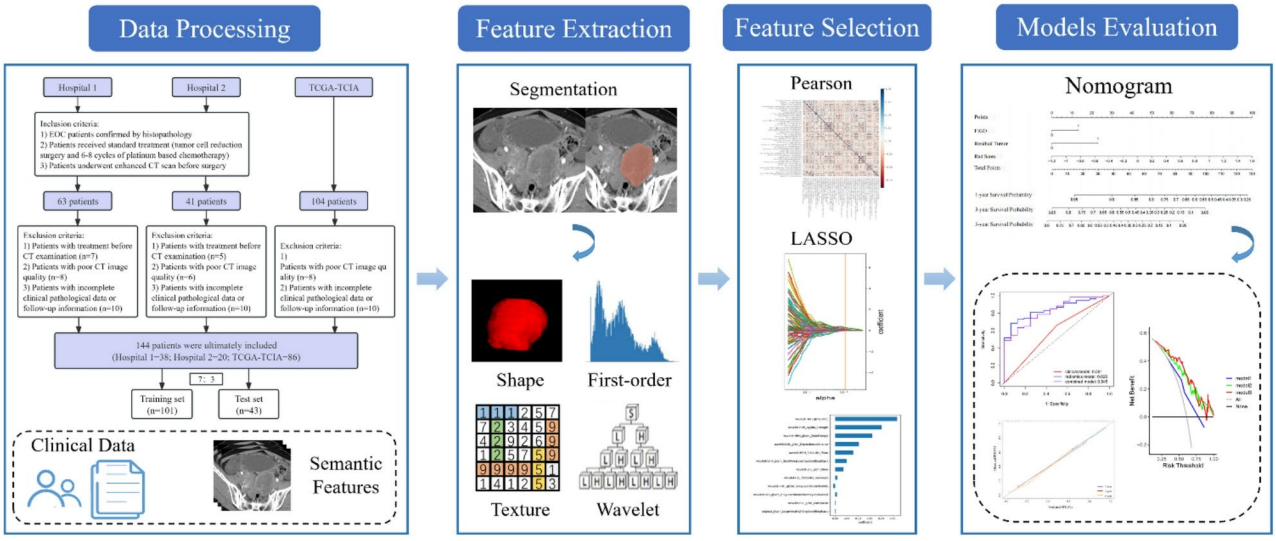

Fig. 1 The workflow of whole study. The workflow consists of four main steps: Data collection and preprocessing, which involves the acquisition of CT images and clinical pathological data; Image segmentation and feature extraction, which includes the extraction of four types of features: shape features, first-order features, textural features, and wavelet features; Feature selection, which is performed using Pearson correlation analysis and the LASSO Cox regression algorithm; and Model construction and validation, which includes the development of a nomogram

TCGA-TCIA, The Cancer Genome Atlas and The Cancer Imaging Archive; EOC, epithelial ovarian cancer; CT, computed tomography; LASSO, least absolute shrinkage and selection operator; FIGO, International Federation of Gynecology and Obstetrics; Rad-score, radiomics score

three different CT scanners. The detailed CT equipment parameters can be found in Supplementary A2.

Two radiologists, with 5 and 10 years of experience in pelvic diagnosis respectively, independently analyzed all CT images. The radiologists were unaware of the clinical and pathological findings. The CT semantic features were evaluated including tumor location, diameter, characteristics, enhanced CT values, and ascites. The tumor diameter refers to the longest diameter of the lesion on the maximum cross-section. The tumor characteristics is defined as mainly cystic (less than 1/3 solid component), mixed cystic and solid (one- to two-thirds solid component), and solid (more than 2/3 solid component). For patients with bilateral lesions, the largest tumor side was selected for analysis. When there is disagreement in the evaluation, final results were determined by a radiologist with 30 years of clinical experience.

Tumor segmentation and radiomics feature extraction

All CT images were preprocessed using Python 3.9 software. By using the linear interpolation algorithm, the original images were resampled to voxel sizes of $1.0 \times 1.0 \times 1.0$ mm^3. The gray levels of each volume were normalized to the range of [0,1]. The region of interest segmentation was performed using the open-source software 3D Slicer (version 4.13.0). Radiologist A manually delineates the region of interest layer by layer along the edge of the primary tumor lesion, avoiding blood vessels and calcified areas as much as possible, and covering all possible areas of the target lesion. Intraclass correlation coefficient (ICC) was utilized to evaluate the reproducibility of the segmentation. The specific method can be found in Supplementary A3.

Radiomics features were obtained utilizing the PyRadiomics package. From the original and eight wavelet-filtered images, 851 radiomics features were extracted, comprising 14 shape features, 18 first-order features, 75 textural features (including gray-level run length matrix (GLRLM) features, gray-level dependency matrix (GLDM) features, gray-level co-occurrence matrix (GLCM) features, neighborhood gray-tone difference matrix (NGTDM) features, gray-level size zone matrix (GLSZM) features), and 744 wavelet features.

Radiomics feature selection

A three-step approach was utilized to reduce the dimensionality of radiomics features in the training set. Initially, Z-score normalization was applied to standardize the radiomics features. Second, Pearson correlation analysis was conducted to exclude features with an absolute pearson correlation coefficient ≥ 0.9. Finally, the least absolute shrinkage and selection operator (LASSO) Cox regression algorithm was utilized to further screen the radiomics features, retaining those with non-zero coefficients. The radiomics score (rad-score) for each patient was calculated by taking the linear combination of these selected features.

Models construction and evaluation

The clinical characteristics and CT semantic features (clinical semantic features) were assessed by univariate and multivariate Cox regression analysis. Clinical semantic features with P-value < 0.05 in univariate Cox regression analysis were incorporated into the multivariate Cox regression analysis. The clinical model was constructed using features identified as independent risk factors with a P-value < 0.05 in multivariate Cox regression analysis. Additionally, two other predictive models were developed using multivariate Cox regression: the radiomics model (based solely on the rad-score) and the combined model (incorporating independent risk factors and the rad-score). Finally, a nomogram for predicting PFS was developed based on the combined model, providing a more intuitive tool for survival prediction.

The discrimination of the three models was evaluated using the consistency index (C-index). Time-dependent receiver operating characteristic (ROC) curve analysis was utilized to assess model predictive performance at different follow-up intervals in both training and test sets. The DeLong test was used to assess differences in area under the curve (AUC) values between the models. Decision curve analysis (DCA) was performed to determine the net benefit rates of the models. Calibration curves were used to evaluate the agreement between the predicted and actual results. The workflow of whole study was shown in Fig. 1.

Statistical analysis

Statistical analyses were conducted using SPSS 26.0 and R software (version 4.2.1). Numerical variables were analyzed using the t-test or Mann-Whitney U test, and categorical variables were assessed with the chi-squared test. Univariate and multivariate Cox regression, LASSO-Cox regression analysis, calibration curves, and the C-index were performed using R software. Details of the R analysis are shown in Supplementary A4. A two-sided $P < 0.05$ indicated a statistically significant difference.

Results

Baseline characteristics

A total of 144 EOC patients were included in the study. Among them, 92 patients experienced disease progression during follow-up, with a median PFS of 557.5 days (range: 9-2154 days). In contrast, 52 patients did not show progression, with a median PFS of 1309.5 days (range: 92-3500 days). The clinical characteristics and CT semantic features of the training and test sets were presented in Table 1. There were no significant differences between the two sets. The median PFS of the training set was 596 days, while it was 869 days in the test set ($P = 0.457$).

Univariate Cox regression analysis revealed that age, menopausal status, stage, and residual tumor were significantly correlated with PFS in the training set. Multivariate Cox regression analysis further demonstrated that stage and residual tumor were significantly correlated with PFS, serving as independent risk factors for predicting disease progression in EOC patients (Table 2). The Kaplan-Meier survival curves for these independent risk factors (stage and residual tumor) indicated that both factors could predict poor prognosis (Fig. 2). Patients with advanced-stage and residual tumor larger than 1 cm had lower PFS (Log-rank test, both $P < 0.05$).

Radiomics feature selection and model construction

A total of 851 radiomics features were extracted from CT images. After Pearson correlation analysis, 266 features remained. Finally, twelve features with non-zero coefficients were selected by the LASSO Cox regression, including one original feature and eleven wavelet-transformed features (Figure S1). The twelve features and their corresponding coefficients are shown in Table 3. Wavelet-HHH_glcm-Imc was the feature most significantly correlated with predicting PFS. The rad-score for each patient in both the training and test sets was shown in Figure S2 The specific calculation formula for the rad-score is provided in Supplementary A5.

The optimal cut-off value of the rad-score, calculated using the Youden index, was − 0.066. In the training set, patients were divided into two groups based on this cut-off value: the high rad-score group and the low rad-score group. Kaplan-Meier analysis was used to validate the prognostic difference between the two groups (Figure S3). The Log-rank test indicated a significant difference between the high and low rad-score groups ($P < 0.001$). Our findings indicate that a higher rad-score is associated with reduced PFS, suggesting its potential as a predictor of poor prognosis.

Models evaluation

Table 4 displays the C-indices for the three models predicting PFS. The combined model exhibited higher prognostic performance than the other models, with C-indices of 0.78 (95% CI: 0.689–0.889) in the training set and 0.73 (95% CI: 0.572–0.886) in the test set. The ROC curves for 1-, 3-, and 5-year PFS were shown in Fig. 3. The combined model outperformed the clinical and radiomics models in predicting 1-, 3-, and 5-year PFS, with AUCs of 0.850 (95% CI: 0.722–0.943), 0.828 (95% CI: 0.722–0.901), and 0.845 (95% CI: 0.722–0.943), respectively. The radiomics model surpassed the clinical model in predicting 1-, 3-, and 5-year PFS, with AUCs of 0.779 (95% CI: 0.757–0.934), 0.812 (95% CI: 0.739–0.917), and 0.826 (95% CI: 0.670–0.889), respectively. Figure 4 presented the DCA for the three models

Table 1 Baseline characteristics of EOC patients in the training and test sets

Characteristics	All patients ($n=144$)	Training set ($n=101$)	Test set ($n=43$)	*P*-value
Age (years)	57.0 (50.0, 66.8)	58.0 (50.0, 67.5)	54.0 (49.0, 63.0)	0.111
Menopause				0.495
Yes	106 (73.6%)	76 (75.2%)	30 (69.8%)	
No	38 (26.4%)	25 (24.8%)	13 (30.2%)	
FIGO stage				0.281
I-II	34 (23.6%)	22 (21.8%)	13 (30.2%)	
III-IV	110 (76.4%)	79 (78.2%)	30 (69.8%)	
CA125 (U/mL)	375.9 (166.0, 719.2)	733.2 (264.1, 1396.5)	673.0 (224.9, 1720.0)	0.991
Residual tumor				0.132
> 1 cm	84 (58.3%)	63 (62.4%)	21 (48.8%)	
≦1 cm	60 (41.7%)	38 (37.6%)	22 (51.2%)	
Tumor location				0.133
Bilateral	94 (65.3%)	62 (61.4%)	32 (74.4%)	
Unilateral	50 (34.7%)	39 (38.6%)	11 (25.6%)	
Tumor diameter (mm)	79.3 (56.1, 114.8)	78.6 (53.5, 113.0)	86.3 (60.0, 116.0)	0.482
Ascites				0.083
Yes	122 (84.7%)	89 (88.1%)	33 (76.7%)	
No	22 (15.3%)	12 (11.9%)	10 (23.3%)	
Tumor characteristics				0.400
Mainly cystic	34 (23.6%)	24 (23.8%)	10 (23.3%)	
Solid	64 (44.4%)	48 (47.5%)	16 (37.2%)	
Mixed cystic and solid	46 (32.0%)	29 (28.7%)	17 (39.5%)	
Enhanced CT value	61.5 (53.6, 67.0)	61.5 (52.8, 66.6)	61.4 (54.6, 68.9)	0.389
Disease progression				0.841
Yes	92 (63.9%)	64 (63.4%)	28 (65.1%)	
No	52 (36.1%)	37 (36.6%)	15 (34.9%)	
PFS (days)	642.5 (320.0, 1296.0)	596.0 (269.5, 1324.0)	869.0 (363.0, 1297.0)	0.457

EOC, epithelial ovarian cancer; FIGO, International Federation of Gynecology and Obstetrics; CA125, carcinoma antigen 125; CT, computed tomography; PFS, progression-free survival

Table 2 Univariate and multivariate Cox regression analysis for predicting PFS in EOC patients

Characteristics	Univariate Cox regression			Multivariate Cox regression		
	HR	95% CI	*P*-value	HR	95% CI	*P*-value
Age	1.027	(1.007–1.048)	0.007	1.006	(0.979–1.035)	0.659
Menopause	0.554	(0.333–0.920)	0.022	0.677	(0.340–1.348)	0.267
FIGO stage	0.495	(0.292–0.839)	0.009	0.576	(0.336–0.989)	0.045
CA125	1.000	(1.000-1.001)	0.062			
Residual tumor	0.374	(0.243–0.575)	< 0.001	0.455	(0.288–0.718)	0.001
Tumor location	1.207	(0.774–1.883)	0.406			
Tumor diameter	1.004	(0.999–1.009)	0.142			
Ascites	0.695	(0.379–1.275)	0.239			
Tumor characteristics						
Mainly cystic	NA		NA			
Solid	1.104	(0.631–1.930)	0.728			
Mixed cystic and solid	1.231	(0.763–1.987)	0.395			
Enhanced CT value	0.982	(0.962–1.001)	0.067			

PFS, progression-free survival; EOC, epithelial ovarian cancer; FIGO, International Federation of Gynecology and Obstetrics; CA125, carcinoma antigen 125; CT, computed tomography; HR, hazard ratio

in predicting 3-year PFS. The DCA demonstrated that the net benefit of the combined model is significantly greater than that of the radiomics and clinical models at different threshold probabilities. The nomogram for predicting PFS is shown in Fig. 5A. To use this nomogram, determine the value of each variable, draw a vertical line straight upward to the point axis to obtain the corresponding score, repeat this process for each variable, sum the scores, and then locate the total score on the Total Points axis to assess the patient's 1-year, 3-year, and

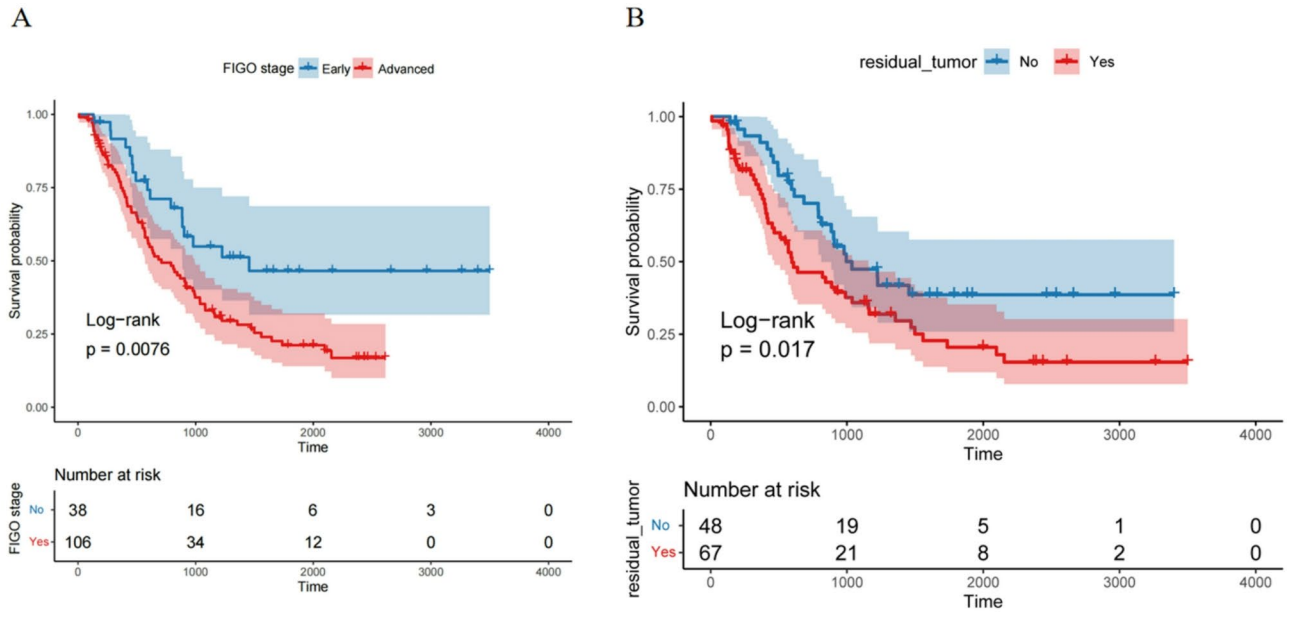

Fig. 2 Kaplan-Meier survival curves of the independent risk factors. (**A**) showed the Kaplan-Meier survival curve of International Federation of Gynecology and Obstetrics stage. (**B**) showed the Kaplan-Meier survival curve of residual tumor

Table 3 Radiomics features retained by LASSO Cox regression

Radiomics features	Coefficients
original_glszm_LargeAreaHighGrayLevelEmphasis	0.001542914
wavelet-HLL_glcm_Correlation	0.002961573
wavelet-LHH_glszm_GrayLevelNonUniformityNormalized	0.007430689
wavelet-HHH_glszm_GrayLevelNonUniformity	-0.00834827
wavelet-HLL_firstorder_Skewness	0.009159909
wavelet-LHL_glcm_Idmn	0.03540515
wavelet-LHH_glszm_SmallAreaLowGrayLevelEmphasis	0.049581306
wavelet-HHH_firstorder_Mean	0.078204555
wavelet-LHL_gldm_DependenceVariance	0.103301648
wavelet-HHH_glszm_ZoneEntropy	0.161251759
wavelet-HHH_ngtdm_Strength	0.202476403
wavelet-HHH_glcm_Imc1	0.270314762

LASSO, least absolute shrinkage and selection operator

Table 4 C-index values of predicting PFS for three models in the training and test sets

Models	Training set		Test set	
	C-index	95% CI	C-index	95% CI
Clinical model	0.61	0.444–0.717	0.61	0.420–0.688
Radiomics model	0.73	0.679–0.757	0.70	0.493–0.724
Combined model	0.78	0.689–0.889	0.73	0.572–0.886

C-index, concordance index; PFS, progression-free survival

5-year PFS risk. The calibration curves for predicting 1-, 3-, and 5-year PFS were approximately on the diagonal, indicating good model calibration (Fig. 5B and C).

Discussion

In this study, we developed and validated an enhanced CT-based radiomics model that incorporates clinical semantic features and the rad-score to predict PFS in patients with EOC. The combined model demonstrated superior predictive performance, with a C-index of 0.78 (95% CI: 0.689–0.889) in the training set and 0.73 (95% CI: 0.572–0.886) in the test set. The radiomics nomogram can assist clinical doctors in formulating personalized treatment plans.

Complete tumor resection is crucial for the prognosis of advanced high-grade serous ovarian cancer (HGSOC) patients and is a primary objective in the initial comprehensive staging of ovarian cancer [19]. The prognosis of FIGO stage IV patients who undergo complete macroscopic resection is better than that of stage IIIC residual tumor patients, indicating that achieving complete resection of tumors to microscopic residuals significantly improves the prognosis of EOC patients [20]. In our study, we identified that residual tumor significantly impacts patients' PFS. Larger residual tumor may reflect greater tumor invasiveness and poorer treatment responses, leading to a reduced PFS. Therefore, strategies aimed at controlling or removing residual tumor after surgery may play a vital role in improving patient prognosis and extending PFS. In this review study, approximately 60% of long-term survivors did not achieve

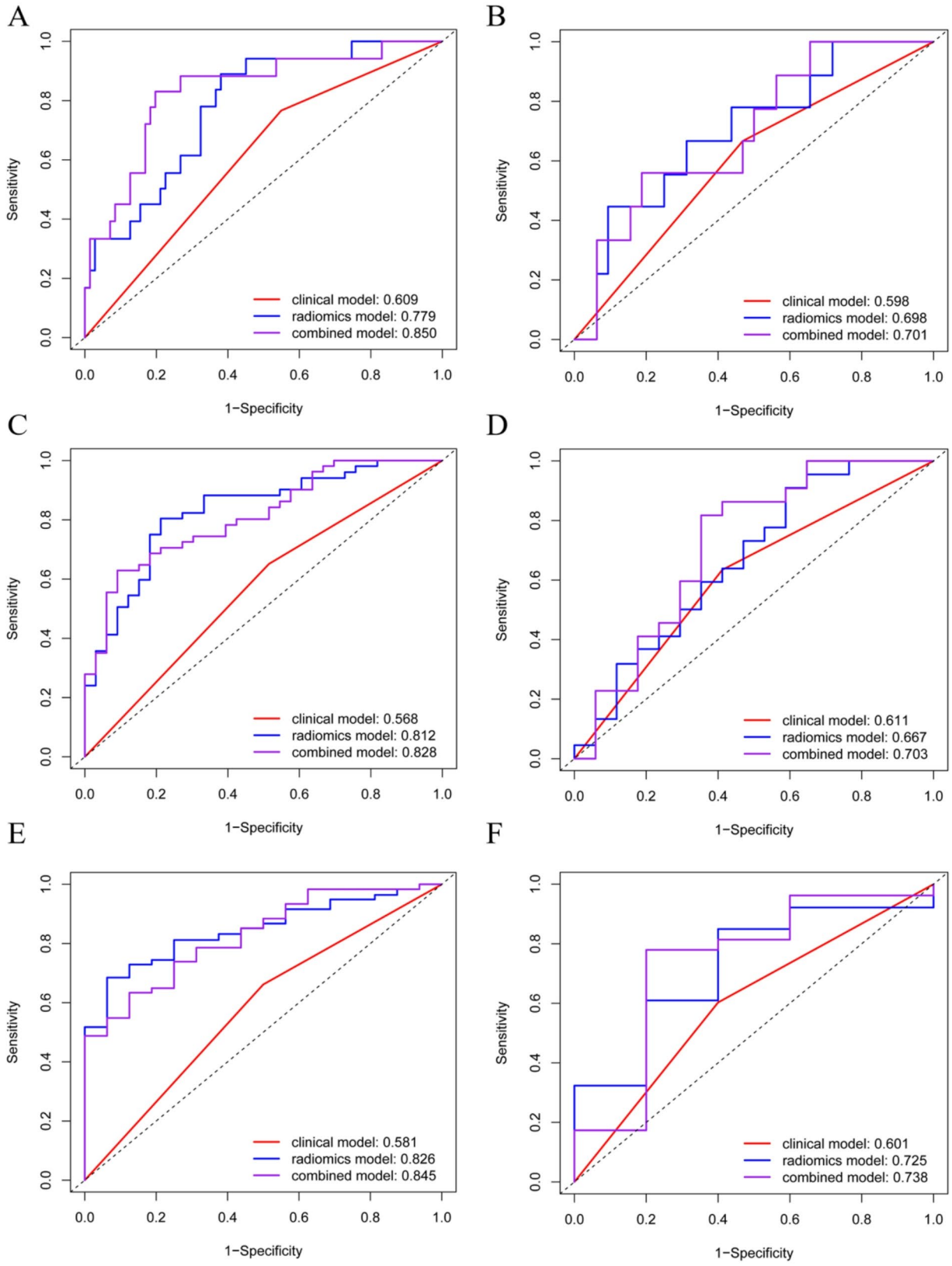

Fig. 3 Receiver operating characteristic (ROC) curves of three models for predicting progress-free survival (PFS). (A-B) showed the ROC curves for predicting 1-year PFS in the training set (**A**) and test set (**B**). (**C**-**D**) showed the ROC curves for predicting 3-year PFS in the training set (**C**) and test set (**D**). (**E**-**F**) showed the ROC curves for predicting 5-year PFS in the training set (**E**) and test set (**F**)

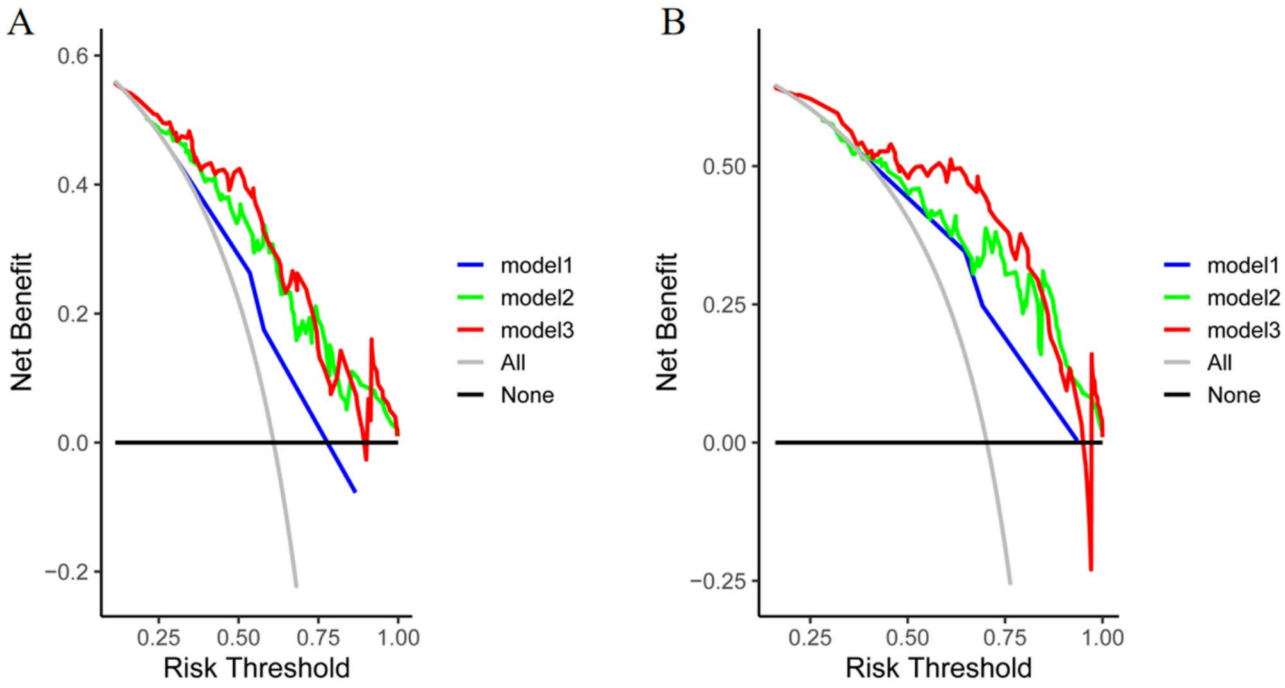

Fig. 4 Decision curve analysis (DCA) for predicting 3-year predicting progress-free survival. (**A**-**B**) showed the DCA of three models in the training set (**A**) and test set (**B**). Model 1 represents the clinical model, Model 2 represents the radiomics model, and Model 3 represents the combined model

complete macroscopic resection at initial surgery, indicating that factors other than residual tumor also influence long-term survival in EOC patients [21]. Many researchers believe that FIGO staging is significantly associated with the prognosis of EOC, with notable differences in PFS between early and advanced stages [22, 23]. In our study, we observed a significant difference in the median PFS between early and advanced-stage EOC patients, with early-stage patients exhibiting a substantially higher PFS compared to their advanced-stage counterparts. This finding is consistent with existing literature, which underscores the importance of early diagnosis and treatment in improving PFS rates. Early-stage patients typically present with a lower tumor burden and a relatively homogeneous tumor microenvironment, which may contribute to their longer PFS. Overall, the results of this study emphasize the crucial role of early diagnosis and tumor residue in PFS of EOC patients, providing strong references for clinical treatment strategies.

The relationship between biological characteristics and radiomic features is complex, making it challenging to elucidate the connection between individual radiomic features and biological pathological development. Therefore, it is necessary to develop a model incorporating multiple features to elucidate the relationship between radiomic features and pathological outcomes [24]. The radiomic features included in the modeling of this study primarily consist of wavelet-transformed GLCM features. Wavelet-transformed features contain more information and can reflect tumor heterogeneity. Wavelet transformation can more accurately represent information at different scales in the image, thereby enhancing the interpretability and reliability of the data [25]. Features obtained through wavelet transformation are more effective in conveying information about intratumoral heterogeneity [26]. In this study, the feature most significantly associated with predicting PFS in EOC patients was wavelet-HHH_glcm_Imc. GLCM features reflect the spatial distribution of voxel intensities, characterizing intratumoral heterogeneity. An increase in GLCM_Imc values may indicate enhanced adhesion between tumor cells or mesenchymal remodeling, which could influence PFS by promoting local infiltration or metastasis [27]. Therefore, the wavelet-HHH_glcm_Imc feature may indirectly reflect the biological invasiveness of tumors by quantifying the dynamic balance between heterogeneity and structural order within the tumor microenvironment, thus providing a potential marker for predicting the progression risk of EOC.

Radiomics involves the extraction of a large number of quantitative features from medical imaging to establish associations between these features and clinical or biological data [28]. In ovarian cancer research, imaging techniques such as CT and positron emission tomography (PET)/CT are widely utilized for the quantitative evaluation of tumors. It is widely acknowledged that high genomic heterogeneity is linked to reduced PFS [29, 30]. In recent years, several studies have explored

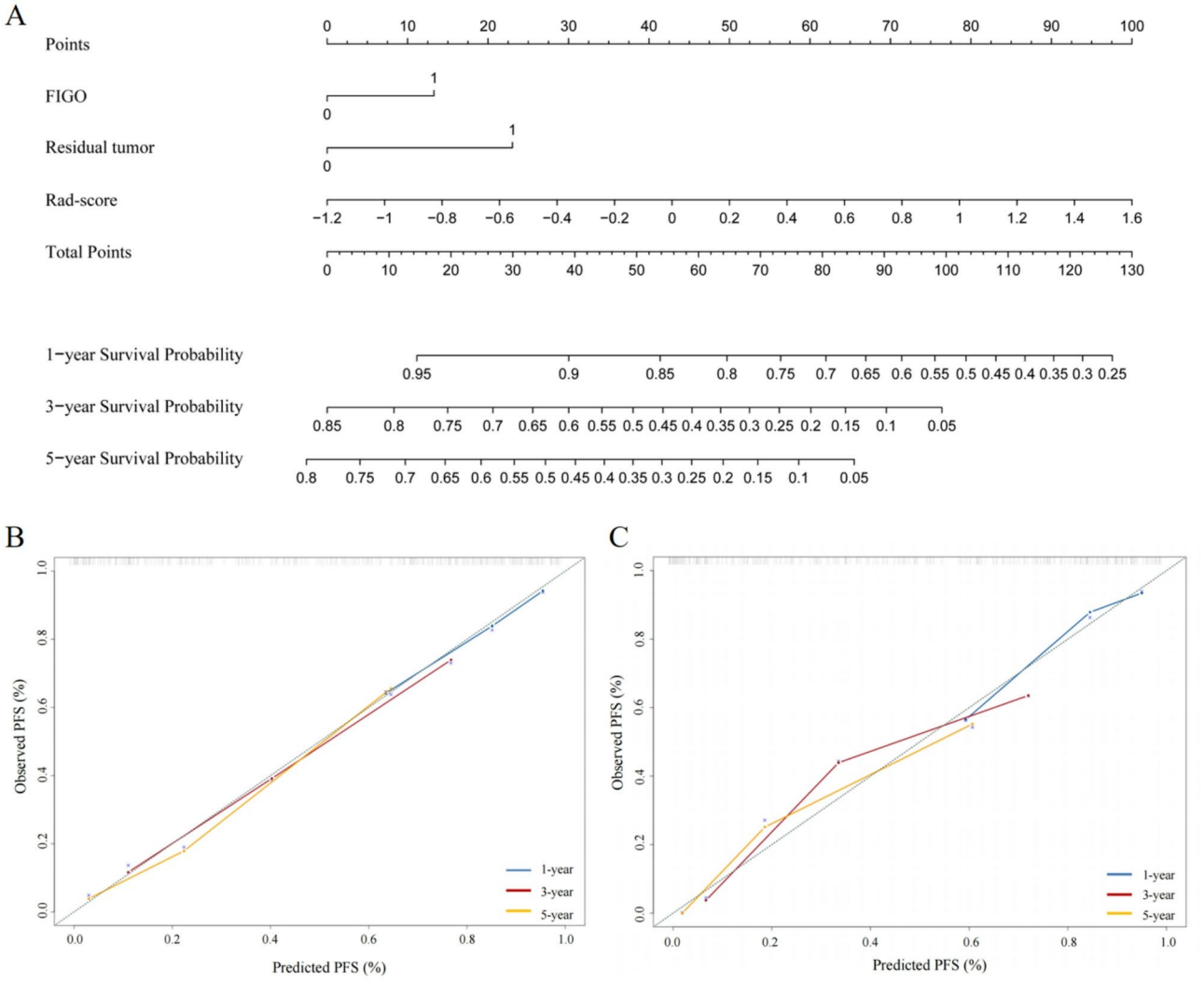

Fig. 5 Radiomics nomogram and its calibration curves for predicting PFS. Nomogram for predicting PFS in epithelial ovarian cancer patients (**A**). The calibration curves for predicting 1-year, 3-year, and 5-year PFS in training set (**B**) and test set (**C**). The blue, red, and orange solid lines represent the consistency between the predicted risk probabilities and the actual probabilities for 1-year, 3-year, and 5-year PFS, respectively
FIGO, International Federation of Gynecology and Obstetrics; Rad-score, radiomics score; PFS, progress-free survival

the relationship between CT radiomic features and patient prognosis, demonstrating that texture analysis of CT scans holds potential in predicting overall survival (OS) in ovarian cancer patients [30–32]. Meier et al. [31] reported that the similarity entropy derived from machine learning models is significantly correlated with longer OS, while the inter-center texture heterogeneity index is notably associated with longer PFS. Wei et al. [32] performed a retrospective analysis of 94 ovarian cancer cases and found that CT radiomic features were closely related to the recurrence of advanced ovarian cancer. Vargas et al. [33] utilized texture indices across 12 sites to capture the heterogeneity of tumor lesions in preoperative CT images of 38 HGSOC patients, revealing that indices representing differences in texture similarity across different sites were associated with shorter OS and incomplete surgical resection. Furthermore, studies have demonstrated that radiomic features extracted from PET/CT images can be used to quantitatively assess metabolic heterogeneity within tumors [34]. Although some small-scale studies have highlighted the predictive value of CT radiomics in ovarian cancer, the comparability of results is limited by the variability in imaging data, which originates from different centers, with inconsistent equipment and scanning protocols. Our multi-center study addresses these challenges, offering a more robust analysis that mitigates the impact of varying devices and scanning protocols. Moreover, we integrated clinical semantic features with radiomic features into a predictive model, significantly enhancing the predictive performance for PFS.

Nomograms provide a more precise individualized prognostic risk assessment in an intuitive graphical manner, enabling clinicians to make personalized treatment decisions, and thus have significant application value in clinical practice. Lin et al. [35] developed and validated a nomogram combining the rad-score and carcinoembryonic antigen levels, showing good discrimination in predicting the T stage of rectal cancer. In this study, a nomogram incorporating FIGO stage, residual tumor, and rad-score was constructed to formulate postoperative adjuvant treatment plans and appropriate follow-up schedules for EOC patients. If the nomogram indicates a low risk of progression, especially when the tumor is located in a surgically accessible position, initial cytoreductive surgery followed by platinum-based chemotherapy would be considered [36]. For patients with a high risk of progression, neoadjuvant chemotherapy followed by interval cytoreductive surgery is recommended. Although this method may positively impact improving quality of life and extending survival, several challenges remain in its clinical implementation. One potential barrier is the clinical acceptance of the tool. To overcome this, we propose providing training sessions to familiarize clinicians with the nomogram and demonstrate its practical benefits. Additionally, ensuring that the tool is user-friendly and integrated into existing clinical workflows will enhance its adoption. Another challenge is the availability and accuracy of CT imaging data. Standardization of image acquisition and analysis protocols is essential to maintain consistency and reliability across different clinical settings. To mitigate this, we recommend developing guidelines for image processing and providing automated tools that reduce the potential for human error. Lastly, the integration of the nomogram into clinical decision-making may require additional resources, such as time for data input and interpretation. However, through collaboration with healthcare institutions and integration into electronic health record systems, we believe that these obstacles can be minimized, making the tool more accessible and efficient in daily practice. In conclusion, while there are challenges in implementing the nomogram into clinical practice, addressing these obstacles through standardization, training, and technological integration can significantly improve its clinical utility and pave the way for wider adoption in diverse healthcare settin.

This study has certain limitations. Firstly, although this is a multicenter study, independent external data were not used to validate the generalizability of the model. Future research for clinical application should incorporate additional centers and prospective data. Secondly, the radiomics analysis was based solely on arterial phase CT images, which may affect the accuracy of the results. Future research should incorporate images from different phases for comparative analysis. Lastly, the tumor delineation process used for radiomics feature extraction is manual and time-consuming. To facilitate clinical application, it is necessary to develop semi-automatic or automatic image segmentation techniques.

Conclusions

The combined model, which incorporates enhanced CT radiomic features and clinical semantic features, can preoperatively assess the PFS of EOC patients. The radiomics nomogram accurately forecasts disease progression in EOC patients post-treatment, assisting clinicians in recognizing high-risk individuals and tailoring treatment plans to enhance PFS. A prospective cohort would be required in the future to validate the performance of the model.

Abbreviations

EOC	Epithelial ovarian cancer
PFS	Progress-free survival
CA125	Carcinoma antigen 125
CT	Computed tomography
TCGA-TCIA	The Cancer Genome Atlas and The Cancer Imaging Archive
FIGO	International Federation of Gynecology and Obstetrics
GLRLM	Gray-level run length matrix
GLDM	Gray-level dependence matrix
GLCM	Gray-level co-occurrence matrix
NGTDM	Neighborhood gray-tone difference matrix
GLSZM	Gray-level size zone matrix
LASSO	Least absolute shrinkage and selection operation regression
Rad-score	Radiomics score
C-index	Consistency index
ROC	Receiver operating characteristic curve
AUC	Area under curve
DCA	Decision curve analysis
HGSOC	High-grade serous ovarian cancer
PET	Positron emission tomography
OS	Overall survival

Supplementary Information

The online version contains supplementary material available at https://doi.org/10.1186/s12885-025-14265-y.

Supplementary Material 1

Acknowledgements

Not applicable.

Author contributions

Conception and design: Yinping Leng and Lianggeng Gong. Administrative support: Lianggeng Gong. Provision of study materials or patients: Fengyuan Luo and Wenjie Liu. Collection and assembly of data: Jingjing Zhou. Data analysis and interpretation: Yinping Leng and Fei Peng. Manuscript writing: Yinping Leng, Fei Peng and Lianggeng Gong. Final approval of manuscript: Lianggeng Gong. All authors contributed to the article and approved the submitted version.

Funding

This work was supported by the Jiangxi Provincial Science and Technology Program (202310508). This work was supported by the Hunan Provincial Natural Science Foundation of China (2025JJ81045).

Data availability

The datasets used and analysed during the current study are available from the corresponding author on reasonable request.

Declarations

Ethics approval and consent to participate

The studies involving human participants were reviewed and approved by the Institutional Review Board of the Second Affiliated Hospital of Nanchang University and Jiangxi Cancer Hospital. Since data were evaluated retrospectively, pseudonymously and were solely obtained for treatment purposes, a requirement of informed consent was waived by the Institutional Review Board of the two centers. We confirm that all experiments were performed in accordance with relevant guidelines and regulations.

Consent for publication

Not applicable.

Competing interests

The authors declare no competing interests.

Received: 3 January 2025 / Accepted: 5 May 2025
Published online: 20 May 2025

References

1. Chen W, Zheng R, Baade PD, Zhang S, Zeng H, Bray F, et al. Cancer statistics in China, 2015. CA Cancer J Clin. 2016;66(2):115–32. https://doi.org/10.3322/caac.21338.
2. Sung H, Ferlay J, Siegel RL, Laversanne M, Soerjomataram I, Jemal A, et al. Global Cancer statistics 2020: GLOBOCAN estimates of incidence and mortality worldwide for 36 cancers in 185 countries. CA Cancer J Clin. 2021;71(3):209–49. https://doi.org/10.3322/caac.21660.
3. Bowtell DD, Böhm S, Ahmed AA, Aspuria PJ, Bast RC Jr., Beral V, et al. Rethinking ovarian cancer II: reducing mortality from high-grade serous ovarian cancer. Nat Rev Cancer. 2015;15(11):668–79. https://doi.org/10.1038/nrc4019.
4. Oza AM, Cook AD, Pfisterer J, Embleton A, Ledermann JA, Pujade-Lauraine E, et al. Standard chemotherapy with or without bevacizumab for women with newly diagnosed ovarian cancer (ICON7): overall survival results of a phase 3 randomised trial. Lancet Oncol. 2015;16(8):928–36. https://doi.org/10.1016/s1470-2045(15)00086-8.
5. Oza AM, Cibula D, Benzaquen AO, Poole C, Mathijssen RH, Sonke GS, et al. Olaparib combined with chemotherapy for recurrent platinum-sensitive ovarian cancer: a randomised phase 2 trial. Lancet Oncol. 2015;16(1):87–97. https://doi.org/10.1016/s1470-2045(14)71135-0.
6. Stewart C, Ralyea C, Lockwood S. Ovarian cancer: an integrated review. Semin Oncol Nurs. 2019;35(2):151–6. https://doi.org/10.1016/j.soncn.2019.02.001.
7. Chen Z, Liang Q, Zeng H, Zhao Q, Guo Z, Zhong R, et al. Exosomal CA125 as A promising biomarker for ovarian Cancer diagnosis. J Cancer. 2020;11(21):6445–53. https://doi.org/10.7150/jca.48531.
8. Gong Z, Han S, Zhang C, Zhao H, Xu J, Sun X. Value of serum miR-21, HE4 and CA125 in surveillance for postoperative recurrent or metastatic ovarian cancer. Pak J Med Sci. 2022;38(4Part–II):939–45. https://doi.org/10.12669/pjms.38.4.5158.
9. Forstner R, Sala E, Kinkel K, Spencer JA. ESUR guidelines: ovarian cancer staging and follow-up. Eur Radiol. 2010;20(12):2773–80. https://doi.org/10.1007/s00330-010-1886-4.
10. Expert Panel on Women's Imaging, Kang SK, Reinhold C, Atri M, Benson CB, Bhosale PR, et al. ACR appropriateness Criteria® staging and Follow-Up of ovarian Cancer. J Am Coll Radiol. 2018;15(5S):S198–207. https://doi.org/10.1016/j.jacr.2018.03.015.
11. Nougaret S, Lakhman Y, Gönen M, Goldman DA, Miccò M, D'Anastasi M, et al. High-Grade serous ovarian cancer: associations between BRCA mutation status, CT imaging phenotypes, and clinical outcomes. Radiology. 2017;285(2):472–81. https://doi.org/10.1148/radiol.2017161697.
12. Zheng YM, Chen J, Zhang M, Wu ZJ, Tang GZ, Zhang Y, et al. CT radiomics nomogram for prediction of the Ki-67 index in head and neck squamous cell carcinoma. Eur Radiol. 2023;33(3):2160–70. https://doi.org/10.1007/s00330-022-09168-6.
13. Wang M, Perucho JAU, Hu Y, Choi MH, Han L, Wong EMF, et al. Computed tomographic radiomics in differentiating histologic subtypes of epithelial ovarian carcinoma. JAMA Netw Open. 2022;5(12):e2245141. https://doi.org/10.1001/jamanetworkopen.2022.45141.
14. Liu S, He J, Liu S, Ji C, Guan W, Chen L, et al. Radiomics analysis using contrast-enhanced CT for preoperative prediction of occult peritoneal metastasis in advanced gastric cancer. Eur Radiol. 2020;30(1):239–46. https://doi.org/10.1007/s00330-019-06368-5.
15. Gong J, Bao X, Wang T, Liu J, Peng W, Shi J, et al. A short-term follow-up CT based radiomics approach to predict response to immunotherapy in advanced non-small-cell lung cancer. Oncoimmunology. 2022;11(1):2028962. https://doi.org/10.1080/2162402x.2022.2028962.
16. Park S, Sham JG, Kawamoto S, Blair AB, Rozich N, Fouladi DF, et al. CT Radiomics-Based preoperative survival prediction in patients with pancreatic ductal adenocarcinoma. AJR Am J Roentgenol. 2021;217(5):1104–12. https://doi.org/10.2214/ajr.20.23490.
17. Su Q, Wang N, Wang B, Wang Y, Dai Z, Zhao X, et al. Ct-based intratumoral and peritumoral radiomics for predicting prognosis in osteosarcoma: A multicenter study. Eur J Radiol. 2024;172:111350. https://doi.org/10.1016/j.ejrad.2024.111350.
18. Rizzo S, Botta F, Raimondi S, Origgi D, Buscarino V, Colarieti A, et al. Radiomics of high-grade serous ovarian cancer: association between quantitative CT features, residual tumour and disease progression within 12 months. Eur Radiol. 2018;28(11):4849–59. https://doi.org/10.1007/s00330-018-5389-z.
19. Reid BM, Permuth JB, Sellers TA. Epidemiology of ovarian cancer: a review. Cancer Biol Med. 2017;14(1):9–32. https://doi.org/10.20892/j.issn.2095-3941.2016.0084.
20. Gaillard S, Lacchetti C, Armstrong DK, Cliby WA, Edelson MI, Garcia AA, et al. Neoadjuvant chemotherapy for newly diagnosed, advanced ovarian cancer: ASCO guideline update. J Clin. 2010;22:JCO2402589. https://doi.org/10.1200/JCO-24-02589.
21. Chiofalo B, Bruni S, Certelli C, Sperduti I, Baiocco E, Vizza E. (2019). Primary debulking surgery vs. interval debulking surgery for advanced ovarian cancer: review of the literature and meta-analysis. Minerva medica 10 (4): 330-340. https://doi.org/10.23736/s0026-4806.19.06078-6
22. Ge L, Li N, Yuan GW, Sun YC, Wu LY (2018). Nedaplatin and paclitaxel compared with carboplatin and paclitaxel for patients with platinum-sensitive recurrent ovarian cancer. American journal of cancer research 8 (6): 1074–1082.
23. Vito Andrea C, Uccella S, Sozzi G, Ceccaroni M, Mautone D, Armano G, et al. Primary site disease and recurrence location in ovarian cancer patients undergoing primary debulking surgery vs. interval debulking surgery. Eur J Surg Oncology: J Eur Soc Surg Oncol Br Association Surg Oncol. 2021;47(5):1075–82. https://doi.org/10.1016/j.ejso.2020.09.014.
24. Hu Y, Weng Q, Xia H, Chen T, Kong C, Chen W, et al. A radiomic nomogram based on arterial phase of CT for differential diagnosis of ovarian cancer. Abdom Radiol (NY). 2021;46(6):2384–92. https://doi.org/10.1007/s00261-021-03120-w.
25. Zheng YM, Pang J, Liu ZJ, Yuan MG, Li J, Wu ZJ, et al. A CT-based deep learning radiomics nomogram for the prediction of EGFR mutation status in head and neck squamous cell carcinoma. Acad Radiol. 2024;31(2):628–38. https://doi.org/10.1016/j.acra.2023.06.026.
26. Chen J, Lu S, Mao Y, Tan L, Li G, Gao Y, et al. An MRI-based radiomics-clinical nomogram for the overall survival prediction in patients with hypopharyngeal squamous cell carcinoma: a multi-cohort study. Eur Radiol. 2022;32(3):1548–57. https://doi.org/10.1007/s00330-021-08292-z.
27. Lambin P, Rios-Velazquez E, Leijenaar R, Carvalho S, van Stiphout RG, Granton P, et al. Radiomics: extracting more information from medical images using advanced feature analysis. Eur J Cancer. 2012;48(4):441–6. https://doi.org/10.1016/j.ejca.2011.11.036.
28. Wei W, Liu Z, Rong Y, Zhou B, Bai Y, Wei W, et al. A computed Tomography-Based radiomic prognostic marker of advanced High-Grade serous ovarian Cancer recurrence: A multicenter study. Front Oncol. 2019;9:255. https://doi.org/10.3389/fonc.2019.00255.
29. Bodelon C, Killian JK, Sampson JN, et al. Molecular classification of epithelial ovarian Cancer based on methylation profiling: evidence for survival heterogeneity. Clin Cancer Res. 2019;25(19):5937–46. https://doi.org/10.1158/1078-0432.CCR-18-3720.
30. Macintyre G, Goranova TE, De Silva D, et al. Copy number signatures and mutational processes in ovarian carcinoma. Nat Genet. 2018;50(9):1262–70. https://doi.org/10.1038/s41588-018-0179-8.
31. Meier A, Veeraraghavan H, Nougaret S, Lakhman Y, Sosa R, Soslow RA, et al. Association between CT-texture-derived tumor heterogeneity, outcomes, and BRCA mutation status in patients with high-grade serous ovarian cancer. Abdom Radiol (NY). 2019;44(6):2040–7. https://doi.org/10.1007/s00261-018-1840-5.
32. Wei W, Rong Y, Liu Z, Zhou B, Tang Z, Wang S, et al. Radiomics: a novel CT-Based method of predicting postoperative recurrence in ovarian Cancer.

Annual Int Conf IEEE Eng Med Biology Soc IEEE Eng Med Biology Soc Annual Int Conf. 2018;2018:4130–3. https://doi.org/10.1109/embc.2018.8513351.
33. Vargas HA, Veeraraghavan H, Micco M, Nougaret S, Lakhman Y, Meier AA, et al. A novel representation of inter-site tumour heterogeneity from pre-treatment computed tomography textures classifies ovarian cancers by clinical outcome. Eur Radiol. 2017;27(9):3991–4001. https://doi.org/10.1007/s00330-017-4779-y.
34. Yang B, Zhong J, Zhong J, et al. Development and validation of a radiomics nomogram based on 18F-Fluorodeoxyglucose positron emission tomography/computed tomography and clinicopathological factors to predict the survival outcomes of patients with Non-Small cell lung Cancer. Front Oncol. 2020;10:1042–56. https://doi.org/10.3389/fonc.2020.01042.
35. Lin X, Zhao S, Jiang H, Jia F, Wang G, He B, et al. A radiomics-based nomogram for preoperative T staging prediction of rectal cancer. Abdom Radiol (NY). 2021;46(10):4525–35. https://doi.org/10.1007/s00261-021-03137-1.
36. Kurnit KC, Fleming GF, Lengyel E. Updates and new options in advanced epithelial ovarian Cancer treatment. Obstet Gynecol. 2021;137(1):108–21. https://doi.org/10.1097/AOG.0000000000004173.

Publisher's note